PHYSICAL REVIEW B **83**, 184422 (2011)

Magnetic and magnetoelastic anomalies of an Er_2Co_{17} single crystal in high magnetic fields

A. V. Andreev,[1,*] Y. Skourski,[2] M. D. Kuz'min,[3] S. Yasin,[2] S. Zherlitsyn,[2] R. Daou,[2,4] J. Wosnitza,[2] A. Iwasa,[5] A. Kondo,[5] A. Matsuo,[5] and K. Kindo[5]

[1]*Institute of Physics ASCR, Na Slovance 2, CZ-18221 Prague, Czech Republic*

[2]*Dresden High Magnetic Field Laboratory, Helmholtz-Zentrum Dresden-Rossendorf, D-01314 Dresden, Germany*

[3]*Leibniz-Institut für Festkörper- und Werkstoffforschung, PF 270116, D-01171 Dresden, Germany*

[4]*Max Planck Institute for Chemical Physics of Solids, Nöthnitzer Str. 40, D-01187 Dresden, Germany*

[5]*Institute for Solid State Physics, University of Tokyo, 5-1-5 Kashiwa, Chiba 277-8581, Japan*

(Received 5 January 2011; revised manuscript received 14 March 2011; published 20 May 2011)

A high-field study of magnetization (up to 68 T) and magnetoelastic properties (up to 60 T) of Er_2Co_{17} is reported. The most significant effect, a first-order transition from the collinear ferrimagnetic to a canted state, is observed at about 40 T with $\boldsymbol{H} \parallel [001]$. The transition is accompanied by a prominent magnetization jump as well as by step-wise anomalies of the magnetoelastic properties. Thus, the volume of the crystal reduces by about 4 per mil, while the speed of transverse sound in the [001] direction increases by as much as 5 per mil. At higher temperatures the anomalies gradually become smaller and less sharp before they finally disappear at ~50 K. The anisotropy constants of the Er sublattice and the molecular field thereon have been determined from the magnetization curves.

DOI: 10.1103/PhysRevB.83.184422 PACS number(s): 75.30.Kz, 75.50.Gg, 75.80.+q

I. INTRODUCTION

The intermetallic compound Er_2Co_{17} has been known since the 1960s as an interesting representative of magnetic materials in which localized magnetism of the 4*f* electrons of a rare-earth element R is combined with itinerant magnetism of the 3*d* electrons of an iron group metal T.[1,2] T-rich R-T intermetallics with light rare-earth elements have been extensively studied because of their practical importance as high-performance magnetic materials.[3] In the compounds with heavy R elements (Gd–Tm), the magnetic moments of the R and T sublattices are coupled ferrimagnetically, which reduces considerably the net magnetic moment and, as a consequence, the prospects for applications. In particular, Er_2Co_{17} has a low-temperature spontaneous magnetic moment M_s of about 10 μ_B per formula unit, compared with ~30 μ_B in ferromagnetic R_2Co_{17} compounds with light R. However, the ferrimagnetic R_2T_{17} are of special scientific interest because a high-magnetic field can make the antiparallel magnetic structure unstable and eventually enforce a parallel orientation of the sublattices. The transition into the forced ferromagnetic state provides important information about the strength of the R-T intersublattice exchange interaction, which is largely responsible for the unique magnetic properties of this class of magnetic materials. It is this interaction that connects the large moment of the sublattice T with the moment of the sublattice R, endowed with a strong magnetic anisotropy. The R-T exchange is so strong that it takes many tens of teslas to break the ferrimagnetic ground state.

Er_2Co_{17} is a particularly interesting system because the preferred moment orientation in Er_2Co_{17} is along the sixfold axis of the hexagonal Th_2Ni_{17}-type structure, whereas in most other R_2Co_{17} and R_2Fe_{17} with heavy rare earths the easy direction lies in the basal plane. The field-induced transitions in easy-plane ferrimagnets are well understood. The total number of first-order phase transitions (jumps) is uniquely determined by a single dimensionless parameter, the ratio of the basal-plane anisotropy constant to the intersublattice exchange energy.[4] As against that, the transitions in easy-axis ferrimagnets depend in a nontrivial way on several such parameters.[5] Thus, easy-axis R_2T_{17} ferrimagnets have a more complex high-field behavior as well as being of rare occurrence. In fact, only two other such compounds are known to exist, Tm_2Fe_{17} and Tm_2Co_{17}. The former has never been studied in magnetic fields higher than 20 T, while the latter has been recently found to undergo an unusual direct transition from a ferri- to ferromagnetic state.[6] Hence, it is clear that the high-field behavior of Er_2Co_{17} is quite unlike that of other R_2T_{17} compounds and therefore it deserves special attention.

Earlier high-field work on Er_2Co_{17} has been somewhat fragmentary. A recent paper[7] reported a first-order transition at 40 T, but the experiment had been carried out on oriented powder rather than on a single crystal and limited to just one temperature, $T = 4.2$ K, and one orientation of applied magnetic field along the easy axis $\boldsymbol{c}$.[7] It should be pointed out, however, that single crystals are indispensable for a meaningful study of these strongly anisotropic materials. Still the threshold field of the transition observed in Ref. 7 agrees well with earlier predictions, 42[8] and 39.5 T.[9,10] In Ref. 13 the measurements were performed on a single crystal, yet the available magnetic field ($\leqslant$35 T) was insufficient to induce any phase transitions. Moreover, the crystal investigated in Ref. 13 had a too large spontaneous magnetization $M_s = 11.6\ \mu_B$/f.u. at $T = 0$, while there is a consensus in the literature that it should be about 10 μ_B/f.u. The discrepancy was explained later[11] by assuming that the sample studied in Ref. 13 was off the 2:17 stoichiometry. This is not implausible: the existence of a homogeneity range in this compound is consistent with the scatter of published T_C values from 1175 K[14,15] through 1186[1] and 1194 K[2] to about 1210 K.[16] An alternative explanation would be that the sample in Ref. 13 contained a small amount of Co metal which is visible as a certain spontaneous moment

in the hard-axis magnetization curve. One way or the other, the only set of pulsed-field magnetization curves taken on a quality single crystal of Er_2Co_{17} was published over three decades ago,[15] the maximum field available then being 10 T. Magnetization curves along the ***b*** axis have not been published. With regards to the magnetoelastic properties of Er_2Co_{17}, the magnetostriction was measured on a single crystal only above the temperature of liquid nitrogen (77–300 K) in low-magnetic fields (below 6 T); the magnetostriction constants $\lambda_1^{\alpha,2}$, $\lambda_2^{\alpha,2}$, and $\lambda^{\gamma,2}$ were determined to be of the order of 10^{-5}–10^{-4} (Ref. 17).

In this work the metamagnetic transition and its temperature evolution have been studied on a single crystal of Er_2Co_{17} by measurements of magnetization and magnetoelastic properties (magnetostriction and magnetoacoustic effects) in pulsed magnetic fields up to 60 T (up to 68 T at 4.2 K).

II. EXPERIMENTAL DETAILS

The single crystal of Er_2Co_{17} was prepared by arc melting of a stoichiometric mixture of 99.9% pure metals in a tri-arc furnace on a water-cooled copper crucible under a protective argon atmosphere. For better homogeneity the alloy buttons were turned over several times and then kept in a molten state for about 1 h before pulling the crystal. The crystal was grown from those molten buttons by the Czochralski method at a pulling speed of 10 mm/h using a tungsten rod as a seed. The obtained single crystal was about 4 mm in diameter and 25 mm long. The x-ray backscattering Laue patterns showed its good quality. Phase purity and lattice parameters were determined by the standard x-ray diffractometry on powder prepared from a piece of the crystal. The lattice parameters $a =$ 832.0 pm and $c = 812.1$ pm are in good agreement with the literature.[3,13,15,18,19] The samples for different measurements were shaped as parallelepipeds with surfaces perpendicular to the main axes [100] (a), [120] (b), and [001] (c).

The magnetization curves were measured along the three principal axes at $T = 4.2$ K in pulsed magnetic fields up to 60 T with a pulse duration of 20 ms at the Dresden High Magnetic Field Laboratory. The magnetization was detected by the induction method using a homemade coaxial pick-up coil system. A detailed description of the installation will be published elsewhere.[20] The magnetization along the c axis was also measured at 1.5 K and at higher temperatures up to 100 K.

For the b and c axes the maximum field was extended up to 68 T using the high-field facility at ISSP in Kashiwa. A 10 kV capacitor bank with a total energy of 250 kJ was used as a generation source. The pulse duration amounted to about 7 ms. The inner diameter of the magnet was 10.5 mm, inside was a quartz-glass cryostat with outer and inner diameters of 8 and 5 mm, respectively. The magnetization signal was detected by a pick-up coil system consisting of three coils (A, B, and C) connected in series. These coils had been wound with 0.1-mm-thick tin-doped copper wire. Coil A, which was responsible for picking up the signal, had been wound with 40 turns on a 3.0-mm-diameter bakelite pipe. The background-compensation coil B contained 40 windings and was connected in the opposite sense with respect to coil A in order to cancel out the output voltage induced by the magnetic field. Fine compensation was achieved by using the two-turn coil C in a balancing bridge circuit. The magnetic field was monitored by a field pick-up coil wound on the magnetization pick-up coil A.

All magnetization curves were corrected for demagnetizing field. Absolute values of the magnetization were calibrated using steady-field data obtained in a commercial magnetometer (Quantum Design PPMS-14).

For the ultrasound measurements, two parallel facets perpendicular to the c axis were polished off on both ends of the crystal, 3.26 mm apart from each other. The measurements were performed using a pulse-echo technique[21] in a He-flow cryostat in pulsed magnetic fields up to 60 T. The experiments at $T = 1.5$ K were carried out in longitudinal as well as in transverse geometry. In the former case both the polarization vector ***u*** of the sound wave and the propagation vector ***k*** were parallel to the c axis. In the latter case ***k*** was parallel to the c axis while ***u*** was parallel to the a axis. In each case two piezoelectric film transducers were glued onto the facets, one on each side of the sample. The magnetic field was always applied along the c axis. At $T = 1.5$ K the sound velocity change at the metamagnetic transition $\Delta v/v$ was found to be much larger in the transverse geometry. Therefore, only such geometry was used for the measurements at elevated temperatures (up to 100 K).

The magnetostriction was measured for each direction separately using an optical fiber strain gauge bonded to the surface of the sample with cyanoacrylate epoxy. The strain gauge consists of either a 1- or 2-mm-long fiber Bragg grating (FBG) written into the core of a standard telecommunications fiber, with a peak reflectivity at 1550 nm. The strain-dependent shift of the peak in the reflectivity of the FBG when the fiber is stretched is detected using a high-resolution grating spectrometer with a camera operating at 47 kHz, giving a resolution of better than 10^{-6} in strain in around 210 μs. Full details of the technique are given elsewhere.[22] The fiber diameter is 0.16 mm including polyimide coating. Transmission of sample strain to the fiber is estimated to be in the range 70%–90%. The strains were measured along the b and c axes in fields up to 60 T applied along the c axis.

III. EXPERIMENTAL RESULTS

Figure 1 presents magnetization curves of an Er_2Co_{17} single crystal at $T = 4.2$ K in magnetic fields up to 60 T applied along the crystallographic directions [100] (a axis), [120] (b axis), and [001] (c axis). The c axis is the easy-magnetization direction: after a rapid initial growth to just over 10 μ_B/f.u., the magnetization changes very slowly, reaching 10.5 μ_B/f.u. at a field of 40 T. The spontaneous magnetization M_s determined in the middle of the gently rising part of the curve amounts to 10.3 μ_B/f.u. This is in good agreement with literature (except for Ref. 13, as mentioned in the Introduction). At a critical field of 40.7 T the c-axis magnetization experiences a stepwise increase to about 22 μ_B, followed by a gradual growth at higher fields. At the maximum applied field 60 T the magnetization reaches 33 μ_B/f.u., which is still far below the saturation value expected for a parallel alignment of the Er and Co sublattices, 46.3 μ_B/f.u. The stepwise magnetization rise is attributed to a first-order phase transition induced by the magnetic field.

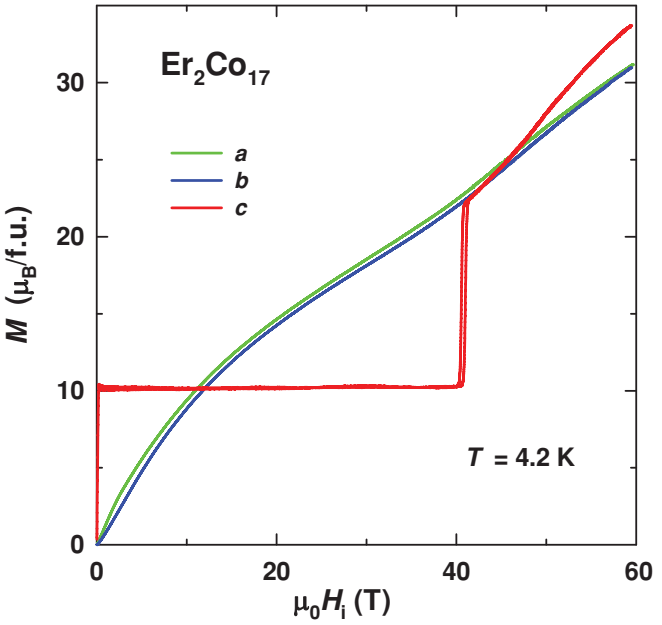

FIG. 1. (Color online) Magnetization curves of an Er_2Co_{17} single crystal measured at $T = 4.2$ K in fields applied along the principal axes.

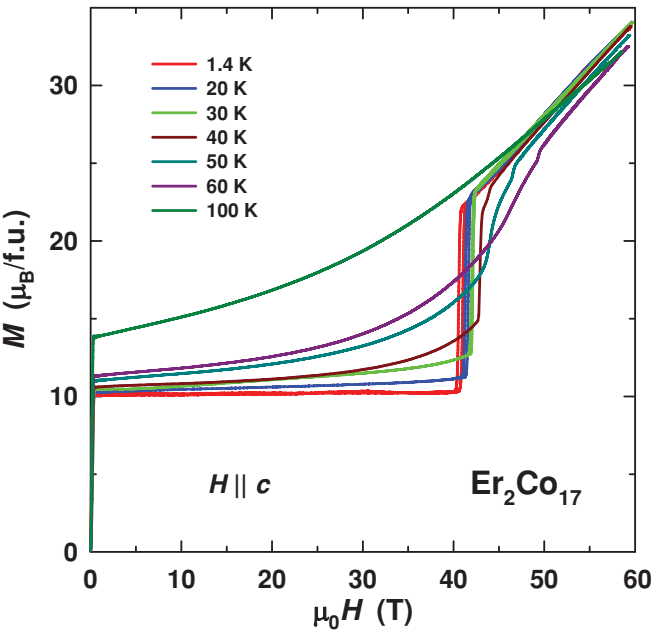

FIG. 2. (Color online) Temperature evolution of the magnetization measured in fields applied along the c axis.

The transition has a hysteresis that is about half a tesla wide. The parameters of the transition, both the critical field H_{cr} and the height of magnetization jump ΔM agree well with the values obtained on aligned powder.[7]

The curves along the two principal directions in the basal plane, the a and b axes, look very similar, except for their initial parts. The higher initial susceptibility and the larger curvature of the magnetization curve along the a axis might be attributed to a less accurate orientation of the crystal during the measurements along this axis, rather than to a magnetic anisotropy within the basal plane. The latter effect ($\approx \sin^6\theta$) can only play a role at higher fields where the angle θ between the Er sublattice moment $\mathbf{M}_{Er}$ and the easy axis $\boldsymbol{c}$ is no longer small. Correspondingly, in the similar compound Tm_2Co_{17} the a- and b-axis magnetization curves were observed to diverge above 20 T only.[6] As far as Er_2Co_{17} is concerned, our data show that the in-plane anisotropy can be neglected up to at least 60 T. The hard- and easy-axis curves intersect at 12 T, neither curve showing any peculiarity at the crossover point. Our value of the crossover field agrees well with earlier studies on single crystals.[12,18]

Figure 2 displays the temperature evolution of the c-axis magnetization. In Fig. 3 the same is shown on an expanded scale in the vicinity of the first-order transition. As the temperature rises, the critical field of the transition H_{cr} increases, whereas the height of the jump ΔM decreases. The width of the hysteresis loop decreases rapidly with temperature and becomes indiscernible ($\sim$0.02 T) at $T = 40$ K. Between 46 and 50 K the first-order transition transforms into an S-shaped curve. At $T = 100$ K the anomaly has disappeared completely. The temperature dependence of the transition parameters is presented in Fig. 4. The spontaneous magnetization M_s obtained in our high-field measurements is in good agreement with earlier data,[15] which confirms the proper calibration of our pulsed-field data. Between 40 and 60 K one can see a small additional anomaly above the main transition (Fig. 3). We have currently no explanation as to the origin of this secondary anomaly and will not discuss it further.

Figure 5 shows the field-dependent changes in the velocity $\Delta v/v$ and attenuation $\Delta\alpha$ of an acoustic wave propagating along the c axis ($\boldsymbol{k} \parallel \boldsymbol{c}$) with either longitudinal ($\boldsymbol{u} \parallel \boldsymbol{c}$) or transverse ($\boldsymbol{u} \parallel \boldsymbol{a}$) polarization at $T = 1.5$ K. In both cases the magnetic field was applied along the c axis. Despite a wide hysteresis caused by instrumental vibrations of the

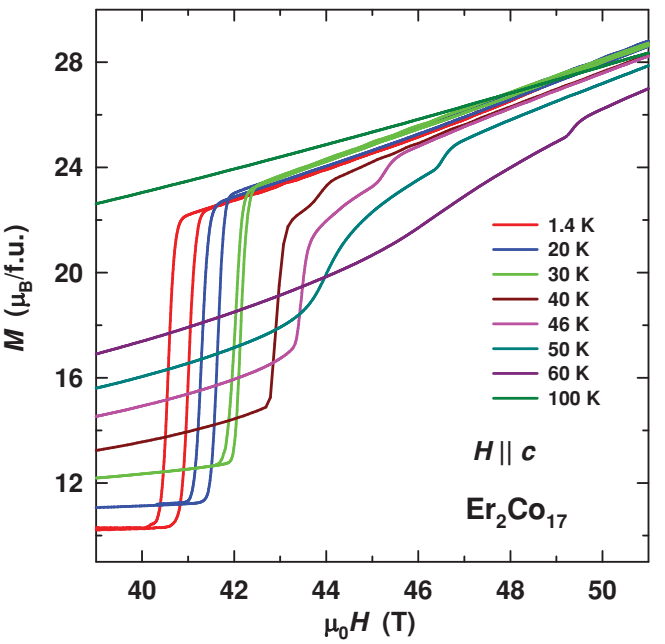

FIG. 3. (Color online) Magnetization for $H \parallel c$ in the vicinity of the metamagnetic transition at different temperatures.

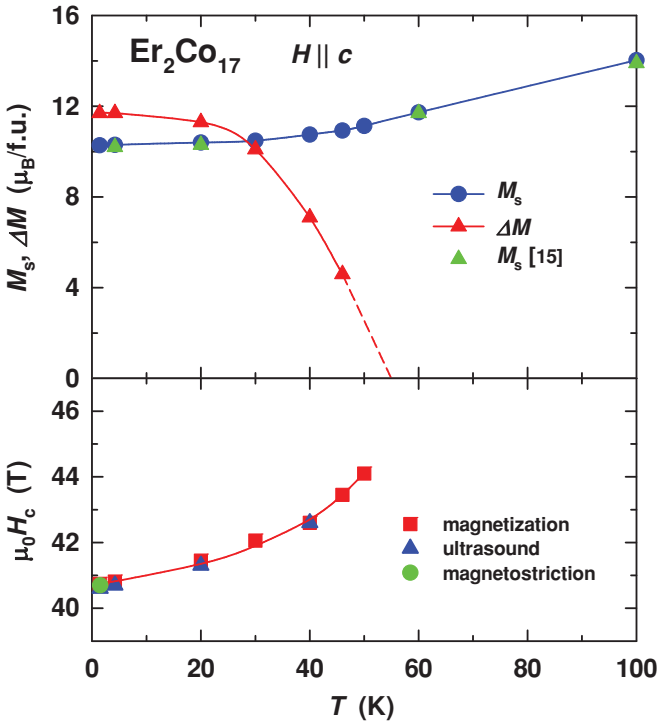

FIG. 4. (Color online) Temperature dependences of the spontaneous magnetization M_s, the magnetization gain ΔM across the metamagnetic transition (upper panel), and the critical field $\mu_0 H_{cr}$ of the metamagnetic transition (lower panel). The $\mu_0 H_{cr}$ values are obtained from the field dependences of the magnetization (squares), changes of the sound velocity (triangles), and jumps in the magnetostriction (circles).

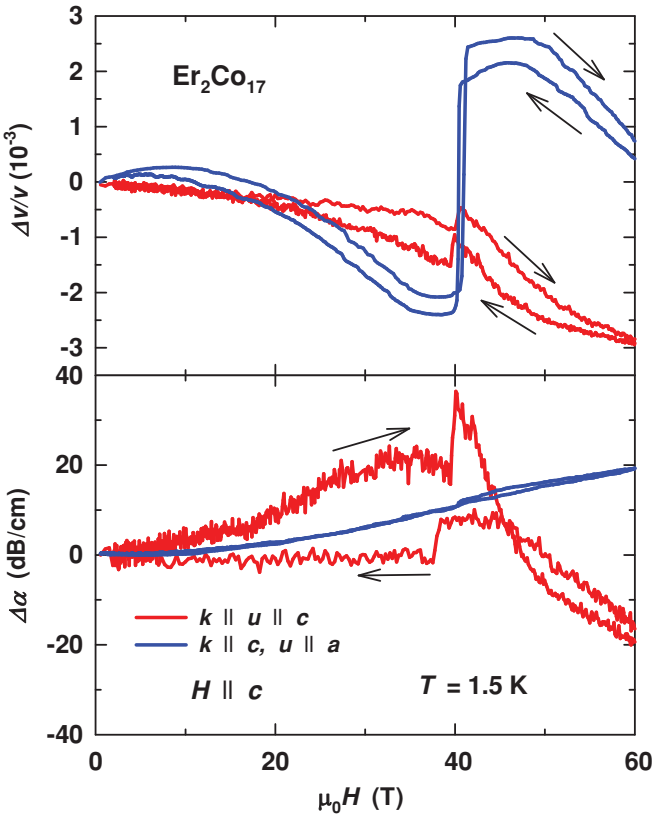

FIG. 5. (Color online) Field dependences of changes in the velocity $\Delta v/v$ and attenuation $\Delta\alpha$ of the acoustic wave propagating along the c axis ($\boldsymbol{k} \parallel \boldsymbol{c}$) in the longitudinal ($\boldsymbol{u} \parallel \boldsymbol{c}$) and transverse ($\boldsymbol{u} \parallel \boldsymbol{a}$) geometry at 1.5 K. The field is applied along the c axis.

sample during the sharp pulse, the first-order transition in the vicinity of 40 T is clearly seen as a step-like anomaly in both geometries. The size of the anomaly in $\Delta v/v$ is considerably larger in the transverse geometry, in agreement with an earlier observation of a similar acoustic anomaly at a spontaneous spin-reorientation transition in the related compound $Er_2(Co_{0.4}Fe_{0.6})_{17}$.[23] The sound attenuation behaves in the opposite way, the effect is almost negligible in the transverse geometry, but shows a large step of $\Delta\alpha \sim 15$ dB cm^{-1} in the longitudinal configuration.

Since the sound velocity is a more fundamental characteristic of a solid than the sound attenuation ($\Delta\alpha$ can be influenced, among other factors, by the quality of the sample, whereas $\Delta v/v$ is an intrinsic property), we selected $\Delta v/v$ in the transverse geometry for a further study of the temperature evolution of the observed effects. The results are displayed in Fig. 6. For clarity of presentation only the falling-field branches of the data are shown (in order to exclude the instrumental hysteresis visible in Fig. 5). The very large jump in $\Delta v/v$ (almost 0.5% at $T = 1.5$ K) decreases monotonically with temperature and vanishes above $T = 60$ K in agreement with the magnetization data. The critical field of the transition, determined as the mean value of the midpoints of the $\Delta v/v$ jumps on rising and falling field, is presented as well in Fig. 4. It coincides very well with the values deduced from the magnetization data. As regards the sound attenuation, the rather small anomaly associated with the first-order transition ($\sim$1 dB/cm at $T = 1.5$ K) vanishes completely above 60 K.

Figure 7 shows the results of the magnetostriction measurements across the metamagnetic transition at 2 K. After an initial increase the linear magnetostriction exhibits a sharp stepwise anomaly at about 40 T. This applies to both the transverse magnetostriction $\Delta l/l_{cb}$ and the longitudinal one $\Delta l/l_{cc}$, where the first subscript refers to the direction of the applied magnetic field and the second one to the direction of the strain measurement. Along the c axis the lattice expands by 0.11×10^{-3}, whereas a contraction by 0.25×10^{-3} is observed along the b axis. The geometry of the measurements is such that the results do not involve the magnetostriction constant λ^{γ}, which describes the difference between the a and b axes in the basal plane. For this reason the volume effect can be evaluated as $\omega = \Delta V/V = 2\,\Delta l/l_{cb} + \Delta l/l_{cc}$ (also shown in Fig. 7). At the transition, a volume shrinkage of $\omega = -0.39 \times 10^{-3}$ is observed.

IV. THEORETICAL MODEL

A. General statements

The behavior of Er_2Co_{17} in strong magnetic fields can be described by means of a two-sublattice model.[24,25] For the case $\boldsymbol{H} \parallel [001]$ the thermodynamic potential can be presented

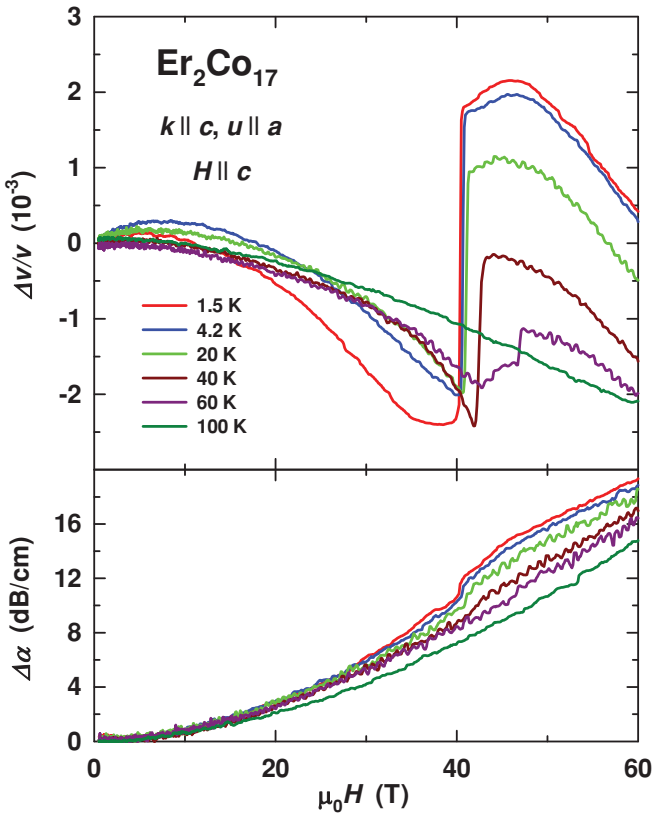

FIG. 6. (Color online) Field dependences of changes in the velocity $\Delta v/v$ and attenuation $\Delta\alpha$ of the acoustic wave propagating along the c axis ($\boldsymbol{k} \parallel \boldsymbol{c}$) in the transverse ($\boldsymbol{u} \parallel \boldsymbol{a}$) geometry at different temperatures. The field is applied along the c axis.

as follows:

$$\Phi = \lambda M_{\mathrm{Co}} M_{\mathrm{Er}} \cos(\alpha+\beta) - \mu_0 H M_{\mathrm{Co}} \cos\alpha - \mu_0 H M_{\mathrm{Er}} \cos\beta + K_1^{\mathrm{Er}} \sin^2\beta + K_2^{\mathrm{Er}} \sin^4\beta + K_3^{\mathrm{Er}} \sin^6\beta. \quad (1)$$

Here λ is an intersublattice exchange constant $\lambda > 0$, α and β are angles between the sublattice magnetizations $\mathbf{M}_{\mathrm{Co}}$ and $\mathbf{M}_{\mathrm{Er}}$, respectively, and the applied magnetic field $\boldsymbol{H}$, and $K_{1,2,3}^{\mathrm{Er}}$ are anisotropy constants of the Er sublattice. The anisotropy within the basal plane has been neglected since no significant difference between the magnetization curves along the $\boldsymbol{a}$ and $\boldsymbol{b}$ axes are observed in Fig. 1. The anisotropy of the Co sublattice has been disregarded altogether because the anisotropy of the isomorphous compound Lu_2Co_{17} is known to be rather weak, $K_1^{\mathrm{Co}} \sim -9$ K/f.u. (-0.6 MJ m^{-3}).[26]

Following Ref. 4 we introduce dimensionless variables

$$\varphi = \frac{\Phi}{\lambda M_{\mathrm{Co}}^2}, \quad h = \frac{\mu_0 H}{\lambda M_{\mathrm{Co}}}, \quad m = \frac{M_{\mathrm{Er}}}{M_{\mathrm{Co}}}, \quad \kappa_n = \frac{K_n^{\mathrm{Er}}}{\lambda M_{\mathrm{Co}}^2}, \quad n = 1,2,3 \quad (2)$$

and rewrite the thermodynamic potential (1) as follows:

$$\varphi(\alpha,\beta) = m\cos(\alpha+\beta) - h\cos\alpha - mh\cos\beta + \kappa_1 \sin^2\beta + \kappa_2 \sin^4\beta + \kappa_3 \sin^6\beta. \quad (3)$$

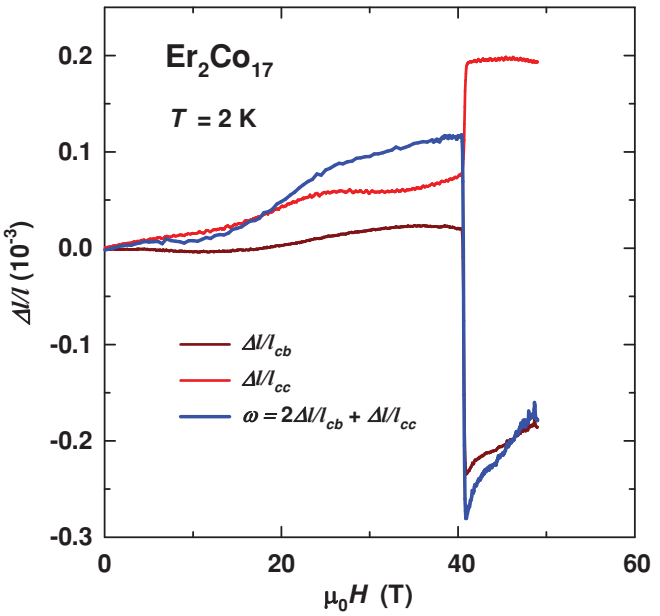

FIG. 7. (Color online) Linear (transverse $\Delta l/l_{cb}$ and longitudinal $\Delta l/l_{cc}$) and volume (ω) magnetostriction of Er_2Co_{17} in fields applied along the c axis at 2 K.

The necessary conditions for equilibrium $\partial\varphi/\partial\alpha = \partial\varphi/\partial\beta = 0$ are given by

$$-m\sin(\alpha+\beta) + h\sin\alpha = 0, \quad (4)$$

$$-m\sin(\alpha+\beta) + mh\sin\beta + 2\kappa_1 \sin\beta\cos\beta + 4\kappa_2 \sin^3\beta\cos\beta + 6\kappa_3 \sin^5\beta\cos\beta = 0. \quad (5)$$

Equations (1), (3), and (5) refer to the case $\boldsymbol{H} \parallel [001]$. Let it now be $\boldsymbol{H} \perp [001]$. Equations (1) and (3) will undergo a slight modification. The anisotropy constants will now be multiplied by even powers of $\cos\beta$ rather than of $\sin\beta$. As a result, Eq. (5) has to be rewritten as follows:

$$-m\sin(\alpha+\beta) + mh\sin\beta - 2\kappa_1 \cos\beta\sin\beta - 4\kappa_2 \cos^3\beta\sin\beta - 6\kappa_3 \cos^5\beta\sin\beta = 0. \quad (5')$$

Whatever the orientation of applied magnetic field, the magnetization projection onto the field direction is given by

$$M_H = M_{\mathrm{Co}}\cos\alpha + M_{\mathrm{Er}}\cos\beta. \quad (6)$$

It is instructive to introduce the reduced magnetization

$$\sigma = \frac{M_H}{M_s} = \frac{\cos\alpha + m\cos\beta}{1-m}. \quad (7)$$

Apparently the reduced magnetization in the easy direction is normalized to unity in weak magnetic fields (i.e., in the limit $h \to 0$, $\alpha \to 0$, $\beta \to \pi$).

B. Determination of model parameters: Sublattice moments and intersublattice exchange field

The low-temperature spontaneous magnetization of Er_2Co_{17}, $M_s = 10.3\ \mu_B$/f.u., is determined directly from the

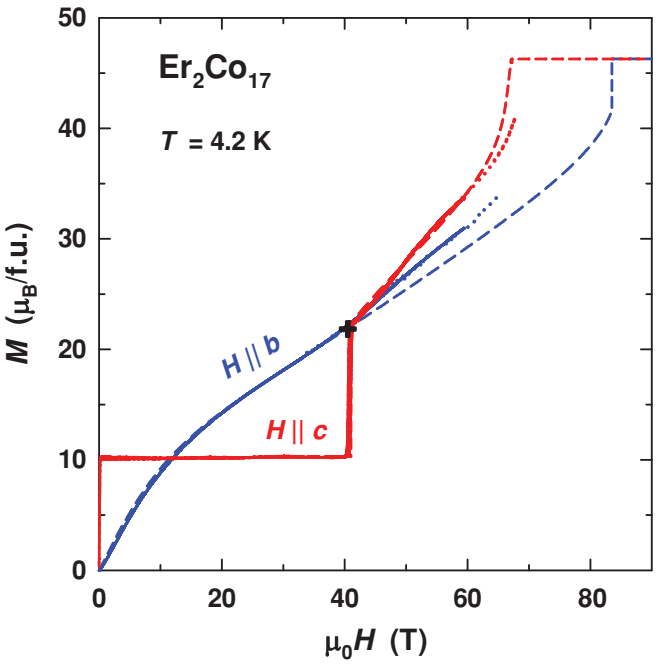

FIG. 8. (Color online) Magnetization curves of Er_2Co_{17}. Solid lines: experiment performed at Dresden. Dotted lines: experimental data obtained at Kashiwa. Dashed lines: calculation. The cross indicates the position of the orthogonality point.

experimental magnetization curve along the easy axis (red curve in Fig. 8) as the mean ordinate of the gently rising part of the curve. The Er magnetic moment determined by polarized-neutron scattering $\mu_{\rm Er} = 8.7(5)\ \mu_B$[27] is consistent with the free-ion value 9 μ_B. Taking $M_{\rm Er} = 2\ \mu_{\rm Er} = 18\ \mu_B$/f.u., we obtain $M_{\rm Co} = M_s + M_{\rm Er} = 28.3\ \mu_B$/f.u. and $m = 18/28.3 = 0.636$.

A general procedure for finding the intersublattice exchange constant consists of locating the so-called orthogonality point in the magnetization curve, that is, such a point where $\beta = \pi/2$.[28] At that point the intersublattice exchange interaction acts in isolation, since the anisotropy terms vanish both in Eqs. (5) and (5'). In the absence of Co anisotropy the ordinate of the orthogonality point is given by[28]

$$M_\perp = \sqrt{M_{\rm Co}^2 - M_{\rm Er}^2} = 21.84\ \mu_{\rm B}/\text{f.u.}$$

This ordinate falls into the discontinuity in the easy-axis magnetization curve (see Fig. 8). Therefore, the orthogonality point should be sought on the prolongation of the continuous high-field part of the red curve to the left of the discontinuity, that is, in the metastable region. In this way we obtain the abscissa $\mu_0 H_\perp = 40.3$ T. The found orthogonality point is marked with a cross in Fig. 8. Alternatively, it could have been determined from the magnetization curve in a hard direction. Both results are identical within error bars, as the cross practically lies on the blue, hard-axis curve in Fig. 8. This is in agreement with the theory[28] which predicts that the orthogonality point should be a crossing point of both magnetization curves, provided the Co anisotropy can be neglected. Thus, our neglect of the latter is corroborated by the data.

For the molecular field on Er we get $\lambda M_{\rm Co} = \mu_0 H_\perp M_{\rm Co}/M_\perp = 52.2$ T.[28] This is 5% higher than what was found in Ref. 14 (50 T) but agrees remarkably well with the value conjectured in Ref. 9 (52.1 T). (Note that the so-called exchange field $H_{\rm ex}$ is a distinct quantity equal to $3\lambda M_{\rm Co}$.)

C. Determination of model parameters: κ_1

The simplest possibility to determine the first anisotropy constant K_1 or κ_1 is to deduce it from the initial slope of the magnetization curve in a hard direction, that is, $\boldsymbol{H} \perp [001]$. Solving simultaneously Eqs. (4) and (5'), wherein α and β are assumed to differ very little from $\pi/2$, one finds the reduced magnetization σ to be proportional to the field h. The proportionality coefficient χ_0, that is, the initial slope of the hard-axis magnetization curve $\sigma(h)$, depends on κ_1 but not on κ_2 or κ_3:

$$\chi_0 = \frac{1-m}{2\kappa_1} + \frac{1}{m(1-m)}. \tag{8}$$

A similar analysis was carried out earlier in Ref. 24; Eq. (6) therein contains the above result (8) as a special case corresponding to $K_1 = K_{12} = 0$, $\eta \ll 1$. Setting $m = 0.636$ in Eq. (8) we find

$$\kappa_1 = \frac{0.182}{\chi_0 - 4.32}. \tag{9}$$

Taking $\chi_0 = 5.15$ from the experiment (Fig. 8) we obtain $\kappa_1 = 0.22$ and $K_1 = \lambda M_{\rm Co}^2 \kappa_1 = 220$ K/f.u. This is in good agreement with the value deduced by Sinnema[13] from magnetization curves measured up to 35 T using a numerical fitting procedure. Our determination of κ_1 from the initial slope has the advantage of being obviously unique.

D. Determination of model parameters: κ_2 and κ_3

As input data we choose the critical field $h_{\rm cr}$ of the jump in the magnetization curve along the c axis and the slope $\chi_\perp$ of the same magnetization curve just above the jump. We take advantage of the proximity of the jump to the orthogonality point (cross in Fig. 8). The conditions of equilibrium [Eqs. (4), (5), and (5')] are expanded in small quantities, deviations from the orthogonality point (see the Appendix for details). The results are the following two restrictions on the anisotropy parameters:

$$\kappa_1 + \kappa_2 + \kappa_3 = (1-m)(1-\sqrt{1-m^2}) + (\sqrt{1-m^2} - 1 + m)(h_{\rm cr} - \sqrt{1-m^2}), \tag{10}$$

$$\kappa_1 + 2\kappa_2 + 3\kappa_3 = \frac{1-m^2}{2} \frac{1-(1-m)\chi_\perp}{1-(1-m)\chi_\perp/m^2}. \tag{11}$$

Note that the subscript of $\chi_\perp$ does not refer to the direction of the field (which in this case is along [001]). Rather, it indicates that the differential susceptibility is taken at the orthogonality point where $M_{\rm Er} \perp \boldsymbol{H}$. Taking from experiment $h_{\rm cr} = 0.78$ and $\chi_\perp = 3.6$ we get

$$\kappa_1 + \kappa_2 + \kappa_3 = 0.09, \tag{10'}$$

$$\kappa_1 + 2\kappa_2 + 3\kappa_3 = 0.04. \tag{11'}$$

TABLE I. Anisotropy constants of the Er sublattice in Er_2Co_{17} at $T = 4.2$ K (K/f.u.). The conversion factor for Er_2Co_{17} is 15 K/f.u. equals 1 MJ m^{-3}.

K_1^{Er}	K_2^{Er}	K_3^{Er}	Source
225	−30	0	Ref. 13
110	−30	0	Ref. 7
220	−210	80	This work

Setting $\kappa_1 = 0.22$, as found in the previous section, in the linear equations (10') and (11') we obtain

$$\kappa_2 = -0.21, \quad \kappa_3 = 0.08. \tag{12}$$

Magnetization curves computed using these parameters are shown as dashed lines in Fig. 8. The values of the anisotropy constants converted to kelvins per formula unit and rounded as appropriate are given in Table I.

V. DISCUSSION

Inspecting Fig. 8 one observes good agreement of the calculated (dashed line) with the Dresden experiment (solid line). In the hard direction the theory slightly lags the experiment at high fields. It should be noted that the lag cannot be eliminated by adjusting the anisotropy parameters κ_1, κ_2, κ_3. Significantly, the calculation predicts a growing upward curvature above 60 T, especially pronounced for $\boldsymbol{H} \parallel \boldsymbol{c}$. Yet, the Dresden data show no upward trend (cf. Fig. 1). In fact, an ever so slight downward curvature may be noticed, if at all. To check the model it was important to extend the field range above 60 T. Such an opportunity became available at the high-field laboratory of the University of Tokyo at Kashiwa where additional data up to 68 T were collected. These are displayed as dotted lines in Fig. 8. An unmistakable upturn is indeed observed in the c-axis curve, as predicted by the model.

The molecular field on Er found in Sec. IV B, $\mu_0 H_{mol} = 52.2$ T, is in good agreement with earlier reports. Overall, there is a consensus as far as H_{mol} in Er_2Co_{17} is concerned. After initially underestimated values of 50 (Ref. 14) and 49.4 T (Ref. 13), practically identical values were given in Ref. 9 (52.1 T)[10] and in Refs. 7 and 28 (52.2 T). Yet, the anisotropy constants appear inconsistent (see Table I). (To avoid confusion, we emphasize that these are anisotropy constants of the Er sublattice in the two-sublattice model.) The anisotropy of the Co sublattice is known to be small, $K_1^{Co} \sim -9$ K/f.u. (-0.6 MJ m^{-3}).[26] Taking this into account has no appreciable effect on the calculated magnetization curves of Er_2Co_{17}[28] and cannot explain discrepancies. On the other hand, the one-sublattice approximation, which regards the two sublattices of a ferrimagnet as rigidly antiparallel, does not apply to R_2Co_{17}.[14,25] In particular, the use of the Sucksmith-Thompson technique[29] should be avoided because it produces strongly underestimated anisotropy constants. Since in the present work the anisotropy constants have been determined by use of a theoretical model rather than by blind fitting of curves, the reasons for the discrepancies between the values in Table I can be elucidated.

In the early work of Sinnema[13] the magnetization curves were measured up to 35 T. The first anisotropy constant was determined in effect so as to satisfy the initial slope condition (8); therefore a correct value of K_1^{Er} was obtained. Sinnema's K_2^{Er} was largely a guess because the available data did not suffice for its reliable determination; K_3^{Er} was arbitrarily set to zero. As a result, Sinnema's higher-order anisotropy constants are incorrect. They do not satisfy the conditions (10') and (11') and do not describe the magnetization jump, of which Sinnema had no knowledge. (N.B.: to obtain the dimensionless parameters κ_i, the K_i^{Er} values in K/f.u. can be conveniently divided by 1000.)

The anisotropy constants found in Ref. 7 are equally wrong. The analysis was limited to just one orientation of applied magnetic field $\boldsymbol{H}\parallel$[001]; the initial slope of the magnetization for with $\boldsymbol{H}\perp$[001] was not considered. As a result, a far too small K_1^{Er} was obtained, which does not satisfy Eq. (8). The anisotropy constants reported in Ref. 7 were in effect chosen to describe the jump of the magnetization in the [001] direction, so the conditions (10') and (11') are fulfilled approximately. To avoid underdetermination in the simultaneous equations (10') and (11'), K_3^{Er} had to be set to zero. Finally, the calculations of Ref. 7 failed to reproduce the upturn observed above 60 T.

Thus the anisotropy constants obtained in Refs. 7 and 13 are incorrect. The former do not describe the initial slope of the basal-plane magnetization curves, whereas the latter fail to explain the discontinuity in the c-axis magnetization. In both cases the lacking information was compensated for by assuming $K_3^{Er} = 0$, even though there is no physical reason for K_3 to be much less than K_1 or K_2 in rare-earth compounds at low temperature.[30]

The volume magnetostriction accompanying the field-induced first-order transition in Er_2Co_{17} is negative. This can be explained in analogy to R_2Fe_{17} compounds. In R_2Fe_{17} the presence of a heavy rare earth enhances the volume anomaly associated with the ferrimagnetic ordering (as compared to Y_2Fe_{17}, Ref. 31, Table 5.2). That is, the R-Fe exchange contributes a volume change of about 10^{-3} with the same sign as the dominant Fe-Fe exchange, whose contribution is $\sim 10^{-2}$. R_2Fe_{17} compounds shrink as the thermal average $\langle\cos(\alpha+\beta)\rangle$ changes from -1 to 0 upon heating from 0 K to the Curie point. So, Er_2Co_{17} should shrink too when the ferrimagnetic structure is abruptly transformed into a canted one and $\cos(\alpha+\beta)$ delivers a (smaller) increment of the same sign, from -1 to about $-m$. The magnitude of the fractional volume change can be estimated as follows:

$$(1-m)\left(\omega_{Er_2Fe_{17}} - \omega_{Y_2Fe_{17}}\right) \sim 0.6 \times 10^{-3}. \tag{13}$$

This estimate with a minus sign has to be compared with the experimental value for Er_2Co_{17}, $\omega = -0.39 \times 10^{-3}$. Not surprisingly, Eq. (13) is an overestimation. This is because the magnetic moment of iron in R_2Fe_{17} (2.1 μ_B) is appreciably larger than the cobalt moment in R_2Co_{17} (1.65 μ_B).

ACKNOWLEDGMENTS

This work has been supported by Grant GACR 202/09/0339 of the Czech Science Foundation and by EuroMagNET under the EU Contract 228043.

APPENDIX: DERIVATION OF EQS. (10) AND (11)

Define small quantities describing deviations from the orthogonality point:

$$\delta = \sin\alpha - m, \tag{A1}$$

$$\varepsilon = \pi/2 - \beta, \tag{A2}$$

$$\eta = h - \sqrt{1-m^2}. \tag{A3}$$

The equilibrium conditions (4), (5), and (5') up to terms linear in the small quantities are as follows:

$$m\eta + \frac{1}{\sqrt{1-m^2}}\delta = m^2\varepsilon, \tag{A4}$$

$$m\eta + \frac{m^2}{\sqrt{1-m^2}}\delta = (m^2 - 2\kappa')\varepsilon, \tag{A5}$$

where

$$\kappa' = \begin{cases} \kappa_1 + 2\kappa_2 + 3\kappa_3, & \mathbf{H}\|[001] \\ -\kappa_1, & \mathbf{H}\perp[001] \end{cases}. \tag{A6}$$

Equation (A5) thus includes both magnetic-field orientations previously described by two separate equations (5) and (5').

From the linear equations (A4) and (A5), δ and η are expressed through ε that is regarded as an independent variable:

$$\delta = \frac{2\kappa'}{\sqrt{1-m^2}}\varepsilon, \tag{A7}$$

$$\eta = m\left[1 - \frac{2\kappa'}{m^2(1-m^2)}\right]\varepsilon. \tag{A8}$$

By use of Eqs. (A3) and (7), the magnetization curve is presented in parametric form as follows:

$$h = \sqrt{1-m^2} + m\left[1 - \frac{2\kappa'}{m^2(1-m^2)}\right]\varepsilon, \tag{A9}$$

$$\sigma = \sqrt{\frac{1+m}{1-m}} + \frac{m}{1-m}\left(1 - \frac{2\kappa'}{1-m^2}\right)\varepsilon. \tag{A10}$$

Hence, one finds the differential susceptibility

$$\chi_\perp = \frac{\partial\sigma}{\partial h} = \frac{\partial\sigma/\partial\varepsilon}{\partial h/\partial\varepsilon} = \frac{1}{1-m}\frac{1-m^2-2\kappa'}{1-m^2-2\kappa'/m^2}. \tag{A11}$$

Solving this equation for κ' and taking the upper case in Eq. (A6), one arrives at Eq. (11).

Finally, Eq. (10) is obtained from the condition of equality of the energies of the phases at the first-order transition point $h = h_{cr}$,

$$m\cos(\alpha+\beta) - h_{cr}\cos\alpha - mh_{cr}\cos\beta + \kappa_1\sin^2\beta + \kappa_2\sin^4\beta + \kappa_3\sin^6\beta = -m - h_{cr} + mh_{cr} \tag{A12}$$

by rewriting it in terms of the small quantities (A1)–(A3).

*Corresponding author: andreev@mag.mff.cuni.cz

[1] R. Lemaire, Cobalt **33**, 201 (1966).

[2] K. Strnat, G. Hoffer, W. Ostertag, and J. C. Olson, J. Appl. Phys. **37**, 1252 (1966).

[3] K. H. J. Buschow, in *Handbook of Magnetic Materials*, edited by K. H. J. Buschow (North Holland, Amsterdam, 1997), Vol. 10, p. 463, and references therein.

[4] M. D. Kuz'min, Y. Skourski, K. P. Skokov, and K.-H. Müller, Phys. Rev. B **75**, 184439 (2007).

[5] M. D. Kuz'min, J. Magn. Magn. Mater. **323**, 1068 (2011).

[6] A. V. Andreev, M. D. Kuz'min, Y. Narumi, Y. Skourski, N. V. Kudrevatykh, K. Kindo, F. R. de Boer, and J. Wosnitza, Phys. Rev. B **81**, 134429 (2010).

[7] S. Yoshii, M. Hagiwara, F. R. de Boer, H. Z. Luo, G. H. Wu, F. M. Yang, and K. Kindo, Phys. Rev. B **75**, 214429 (2007).

[8] J. J. M. Franse, R. J. Radwanski, and S. Sinnema, J. Phys. (Paris) **49**, C-8-505 (1988).

[9] X. F. Han, H. M. Jin, Z. J. Wang, T. S. Zhao, and C. C. Sun, Phys. Rev. B **47**, 3248 (1993).

[10] A "better" prediction was obtained in Ref. 11 on the basis of a rather accurate value of the intersublattice molecular field in Er_2Co_{17}, $\mu_0 H_{mol} = 52.1$ T, which is probably fortuitous. For example, the guess for Gd_2Co_{17} in the same work, $\mu_0 H_{mol} = 194$ T, proved not as successful. A year later inelastic neutron scattering experiments[12] found a value 13% higher, 219 T.

[11] X. F. Han, Q. S. Li, Y. Zhang, J. M. Li, and L. Y. Lin, J. Phys.: Condens. Matter **9**, 7617 (1997).

[12] M. Loewenhaupt, P. Tils, K. H. J. Buschow, and R. S. Eccleston, J. Magn. Magn. Mater. **138**, 52 (1994).

[13] S. Sinnema, Ph.D. Thesis, University of Amsterdam (1988).

[14] N. V. Kudrevatykh, A. V. Deryagin, A. A. Kazakov, V. A. Reimer, and V. N. Moskalev, Phys. Met. Metallogr. **45**(6), 38 (1978).

[15] A. V. Deryagin, N. V. Kudrevatykh, and V. N. Moskalev, Phys. Status Solidi (a) **45**, 71 (1978).

[16] H. Y. Chen, W. W. Ho, S. G. Sankar, and W. E. Wallace, J. Magn. Magn. Mater. **78**, 203 (1989).

[17] A. V. Deryagin, N. V. Kudrevatykh, R. Z. Levitin, and Y. F. Popov, Phys. Status Solidi (a) **51**, K125 (1979).

[18] A. V. Deryagin, N. V. Kudrevatykh, and Y. F. Bashkov, Proc. Int. Conf. Magn. **1**, 222 (1974).

[19] A. Deryagin, A. Ulyanov, N. Kudrevatykh, E. Barabanova, Y. Bashkov, A. Andreev, and E. Tarasov, Phys. Status Solidi (a) **23**, K15 (1974).

[20] Y. Skourski, M. D. Kuz'min, K. P. Skokov, A. V. Andreev, and J. Wosnitza, Phys. Rev. B (in press).

[21] B. Wolf, B. Lüthi, S. Schmidt, H. Schwenk, M. Sieling, S. Zherlitsyn, and I. Kouroudis, Physica B **294-295**, 612 (2001).

[22] R. Daou, F. Weickert, M. Nicklas, F. Steglich, A. Haase, and M. Doerr, Rev. Sci. Instrum. **81**, 033909 (2010).

[23] A. V. Andreyev, A. V. Deryagin, S. M. Zadvorkin, G. M. Kvashnin, and N. V. Kudrevatykh, Phys. Met. Metallogr. **61**(4), 107 (1986).
[24] A. A. Kazakov, V. A. Reimer, A. V. Deryagin, and N. V. Kudrevatykh, Sov. Phys. Solid State **18**, 167 (1976).
[25] A. Sarkis and E. Callen, Phys. Rev. B **26**, 3870 (1982).
[26] E. A. Tereshina and A. V. Andreev, J. Magn. Magn. Mater. **320**, e132 (2008).
[27] O. Moze, R. Caciuffo, B. Gillon, and F. E. Kayzel, J. Magn. Magn. Mater. **104–107**, 1394 (1992).
[28] M. D. Kuz'min, Phys. Rev. **79**, 212405 (2009).
[29] W. Sucksmith and J. E. Thompson, Proc. R. Soc. (London) **225**, 362 (1954).
[30] M. D. Kuz'min and A. M. Tishin, Theory of crystal-field effects in 3d-4f intermetallic compounds, in *Handbook of Magnetic Materials*, edited by K. H. J. Buschow (North-Holland, Amsterdam, 2008), Vol. 17, Chap. 3.
[31] A. V. Andreev, in *Handbook of Magnetic Materials*, edited by K. H. J. Buschow (North-Holland, Amsterdam, 1995), Vol. 8, p. 59.